Nuclear Instruments and Methods in Physics Research B 308 (2013) 9–14

Contents lists available at SciVerse ScienceDirect

Nuclear Instruments and Methods in Physics Research B

journal homepage: www.elsevier.com/locate/nimb

Development of spin-polarized slow positron beam using a ^{68}Ge–^{68}Ga positron source

Masaki Maekawa *, Yuki Fukaya, Atsushi Yabuuchi, Izumi Mochizuki, Atsuo Kawasuso

Advanced Science Research Center, Japan Atomic Energy Agency, 1233 Watanuki, Takasaki, Gunma 370-1292, Japan

ARTICLE INFO

Article history:
Received 4 June 2012
Received in revised form 1 March 2013
Available online 19 April 2013

Keywords:
Slow positron beam
Spin polarized
^{68}Ge
Ion irradiation

ABSTRACT

A ^{68}Ge–^{68}Ga positron source was produced from the ^{69}Ga(p,2n)^{68}Ge nuclear reaction by irradiating a GaN substrate with 20 MeV protons. Fast positrons from the source were converted to slow positrons using tungsten meshes and foils and were then electrostatically transported to the sample chamber. The spin polarization of the positron beam was determined as 47 ± 8% from the magnetic field dependence of the para-positronium intensity in fused silica. The Doppler broadening of the annihilation radiation spectra of polycrystalline Fe showed asymmetry upon field reversal. The spin-polarized positron beam generated by the ^{68}Ge–^{68}Ga source may be applicable to study the magnetic properties associated with surfaces, interfaces, and thin films.

1. Introduction

Positrons emitted from radioisotopes are longitudinally spin-polarized due to the parity non-conservation in the weak interaction. Positron annihilation studies have shown that the ferromagnetic band structure can be investigated using the angular correlation of annihilation radiation (ACAR) technique with spin-polarized positrons [1–3]. More recently, the Doppler broadening of annihilation radiation (DBAR) technique, which in comparison with ACAR has a much simpler experimental setup, may also be suitable for spin-polarized positron annihilation spectroscopy (SP-PAS).

In 1980s, Gidley et al. demonstrated the spin polarization of a slow positron beam generated with a ^{22}Na source. They used the spin-polarized positron beam to the study of surface magnetism of Ni [4]. Subsequently, only a limited number of works have been performed. Considering the fact that various novel spin phenomena have recently been found to occur at surfaces/interfaces and in thin films, spin-polarized positron beams may be useful in spintronics studies [4–12].

In this work, we developed a spin-polarized beam from a ^{68}Ge–^{68}Ga source based on electrostatic beam transport. We describe the numerical simulations used to determine the optimum conditions for generating a spin-polarized positron beam. We then discuss the development of the ^{68}Ge–^{68}Ga source and the spin-polarized positron beam.

2. Preliminary evaluation

2.1. Spin polarization

SP-PAS for surfaces, interfaces, and thin films requires a highly spin-polarized positron beam. The spin polarization of positrons emitted from a positron source into an open angle, θ, in a specific direction is given by

$$P = \frac{v}{c}\frac{1+\cos\theta}{2}, \tag{1}$$

where v is the positron speed and c is the speed of light [13]. The speed term can be rewritten in terms of the kinetic energy, E

$$\frac{v}{c} = \sqrt{1-\frac{1}{[1+E/(mc^2)]^2}}, \tag{2}$$

where m is the static mass of the positron. The average positron spin polarization from a source is given by

$$\langle P\rangle = \frac{\langle v\rangle}{c}\frac{1+\cos\theta}{2} = \int_0^{E_{max}}\sqrt{1-\frac{1}{[1+E/(mc^2)]^2}}N(E)dE\frac{1+\cos\theta}{2}, \tag{3}$$

where $N(E)$ is the energy distribution of positrons and E_{max} is the maximum positron energy. Here, $N(E)$ is not necessarily the same as the energy distribution of the radioisotopes, because $N(E)$ is modified by the energy discrimination of positrons resulting from self-absorption inside the source and absorption in the absorbers and moderators. Also, the open angle, θ, depends on the source

* Corresponding author. Tel.: +81 27 346 9330.
E-mail address: maekawa.masaki@jaea.go.jp (M. Maekawa).

0168-583X/$ - see front matter © 2013 Elsevier B.V. All rights reserved.
http://dx.doi.org/10.1016/j.nimb.2013.04.015

and sample geometry for conventional positron annihilation experiments, and on the source and moderator geometry for slow positron beam generation. Eqs. (1)–(3) suggest that positron sources with a higher energy end-point are better for generating highly spin-polarized positron beams.

Some of the low energy positrons will be absorbed inside the source. The energy spectrum of positrons emitted from the source is given by

$$N_S(E) = \frac{1}{2}\int_0^{d_S} N_0(E)[A(z)/A_0]T_S(E,z)dz, \quad (4)$$

where $N_0(E)$ is the original energy distribution of positrons emitted from nuclei, $A(z)$ is the depth distribution of the source activity, $A_0 = \int_0^{d_S} A(z)dz$, d_S is the source thickness, and $T_S(E,z)$ is the transmission probability of positrons at a depth of z and an energy of E in the source material. If an absorber with a thickness of d_A is placed in front of the source, the energy distribution becomes

$$N_A(E) = N_S(E)T_A(E,d_A), \quad (5)$$

where $T_A(E,d_A)$ is the transmission probability of the positrons. The transmission probability is generally given by

$$T(E,z) = \exp[-(z/z_0)^m], \quad (6)$$

$$z_0 = aE^n/[\rho\Gamma(1+1/m)], \quad (7)$$

where m and n are the material dependent constants, ρ is the material density, and $a = 4.0\ \mu g\ cm^{-2}\ keV^{-n}$. Thus, $T_S(E,z)$ and $T_A(E,d_A)$ can be obtained using appropriate values of m, n, and ρ.

When a slow positron beam is generated using a moderator, positrons with a particular energy distribution are converted to slow positrons. The faster positrons are transmitted without being moderated. Positrons stopped far from the reemission surface annihilate without reaching it. Therefore, the moderator also functions as an absorber to change the positron energy distribution. Thus, for the final positron energy distribution, including the self-absorption in the source, the absorption and the moderation is given by

$$N(E) = N_S(E)T_A(E,d_A)\varepsilon_M(E,d_M), \quad (8)$$

where d_M is the moderator thickness and $\varepsilon_M(E,d_M)$ is the moderator efficiency that is given by

$$\varepsilon_M(E,d_M) = \begin{cases} P_{em}\int_0^{d_M} p(E,z)\sinh(z/L)/\sinh(d_M/L)dz, & \text{transmission type} \\ P_{em}\int_0^{d_M} p(E,z)\exp(-z/L)dz, & \text{reflection type} \end{cases} \quad (9)$$

where P_{em} is the positron branching ratio of reemission into a vacuum and the inner reflection of positrons, $p(E,z)$ is the positron implantation profile ($= -dT(E,z)/dz$), and L is the positron diffusion length [14].

The ^{68}Ge–^{68}Ga source that we produced using a GaN target material has a higher energy end-point (1.9 MeV) than that of ^{22}Na (0.55 MeV). Fig. 1(a) shows the initial energy distribution, $N_0(E)$ [15], the energy distribution of the positrons emitted from the source, $N_S(E)$, and the final energy distribution, $N(E)$. The conditions for these energy distributions are: $A(z)$ shown in the following subsection, $d_S = 0.5$ mm, a GaN target density of $\rho = 6.15\ g/cm^3$, $m = 2.0$, $n = 1.6$, no absorber present, a tungsten moderator assembly composed of transmission and reflection moderators (Fig. 6(a)) where $d_M = 10\ \mu m$, $m = 1.7$, $n = 1.67$, $\rho = 19.3\ g/cm^3$, $P_{em} = 0.33$, and $L = 135$ nm. For comparison, Fig. 1(b) shows $N_0(E)$, $N_S(E)$, and $N(E)$ calculated for a ^{22}NaCl source with a uniform $A(z)$, $d_S = 0.1$ mm, no absorber present, and the same moderator. Consequently, using Eq. (3) with $\theta = 78°$, the spin polarizations of the positron beams for the ^{68}Ge–^{68}Ga/GaN and the ^{22}NaCl sources are estimated to be 53% and 42% respectively. Thus, to generate highly spin-polarized positron beams, it is important to use positron sources with higher energy end-points.

2.2. Source activity

The ^{68}Ge–^{68}Ga and ^{44}Ti–^{44}Sc positron sources have relatively long half-lives and higher energy end-points (288 days and 1.9 MeV, 48 years and 1.5 MeV, respectively) [16]. The cross section of the nuclear reaction ^{45}Sc (p,2n)^{44}Ti is small, whereas the production of ^{68}Ge–^{68}Ga is easier. The stable isotopes of Ga are ^{69}Ga (60.1%) and ^{71}Ga (39.9%). The total amount of ^{68}Ge–^{68}Ga produced by ^{69}Ga(p,2n)^{68}Ge and ^{71}Ga(p,4n)^{68}Ge continuously increases when the proton energy (E_p) increases from 15 to 150 MeV. The net positron intensity emitted from the target is reduced for higher proton energies because ^{68}Ge–^{68}Ga is produced in a deeper region of the target. As shown later, the optimum proton energy for obtaining a high positron emission efficiency from the target surface ranges from 20 to 30 MeV. The cross section of ^{69}Ga(p,2n)^{68}Ge ($0.465 \times 10^{-24}\ cm^2$)) is threefold higher than that of ^{71}Ga(p,4n)^{68}Ge ($0.137 \times 10^{-24}\ cm^2$). High purity ^{69}Ga should be used as a target material; in our preliminary research, molten Ga reacted with the other metal components of the source capsule during irradiation, which eventually destroyed the capsule. To avoid this problem, we propose GaN as a target material, although the amount of ^{69}Ga(p,2n)^{68}Ge is decreased because of the reduced ^{69}Ga content.

Fig. 2(a) shows the depth profile of ^{68}Ge–^{68}Ga in a GaN target simulated by the Induced Radioactivity Analysis Code (IRAC) [17] at various proton energies. The total activity is only half that of the ^{69}Ga target. Assuming a proton current of 3 μA and an irradiation duration of 100 h, the total activities of ^{68}Ge–^{68}Ga are estimated to be 175, 359, and 497 MBq for $E_p = 20$, 25, and 30 MeV, respectively.

The net positron intensity emitted outside from the target is given by

$$I(d_S) = \frac{1}{2}\int_0^{E_{max}}\int_0^{d_S} A(z)T_S(E,z)N_0(E)dzdE. \quad (10)$$

Fig. 2(b) shows the net positron emission rate as a function of target thickness using the depth profiles shown in Fig. 2(a). The greatest positron yield is obtained for $E_p = 25$ MeV and a target thickness of 1 mm. However, the emission efficiency for each total activity is highest for $E_p = 20$ MeV and target thickness of 0.5 mm. The positron beam flux obtained for typical proton beam conditions (3 μA, 100 h) is of the order of $10^4\ e^+/s$. The flux could be enhanced by repeating the proton bombardment because of the long half-life of ^{68}Ge–^{68}Ga. Thus, it is feasible to produce ^{68}Ge–^{68}Ga with a strong enough intensity for generating a positron beam.

3. Development of spin-polarized positron beam

3.1. Source production

Fig. 3 shows schematic diagrams of the source capsule. The target material was a GaN single crystal with a diameter of 8 mm and a thickness of 0.475 mm. To avoid metallization during irradiation, the GaN target was placed in a carbon tray. The tray containing the target was set on an irradiation stage equipped with a water-cooled jacket to protect against heat damage during ion irradiation. The irradiation chamber was evacuated to a base pressure of 5×10^{-4} Pa. The target was directly irradiated with 20 MeV proton beam with a maximum current of 3.5 μA using the cyclotron at the Takasaki Advanced Radiation Research Institute of the Japan Atomic Energy Agency. The efficiency of the source production was estimated to be 0.5 MBq/μA/h from the annihilation gamma ray

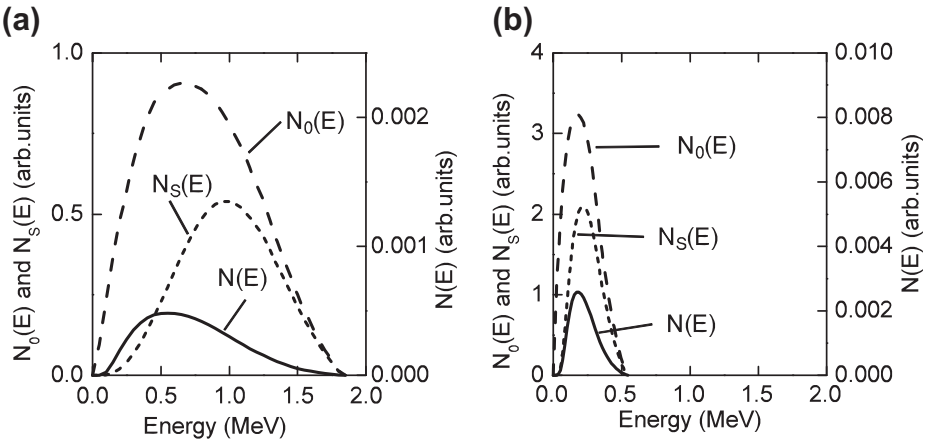

Fig. 1. Calculated energy spectrum of the emitted positrons from the nuclei [$N_0(E)$], from the source surface [$N_S(E)$], and the final energy spectrum [$N(E)$] taking into account the absorption inside the source and moderator shown in Fig. 6(a) for (a) ^{68}Ge–^{68}Ga/GaN and (b) ^{22}Na.

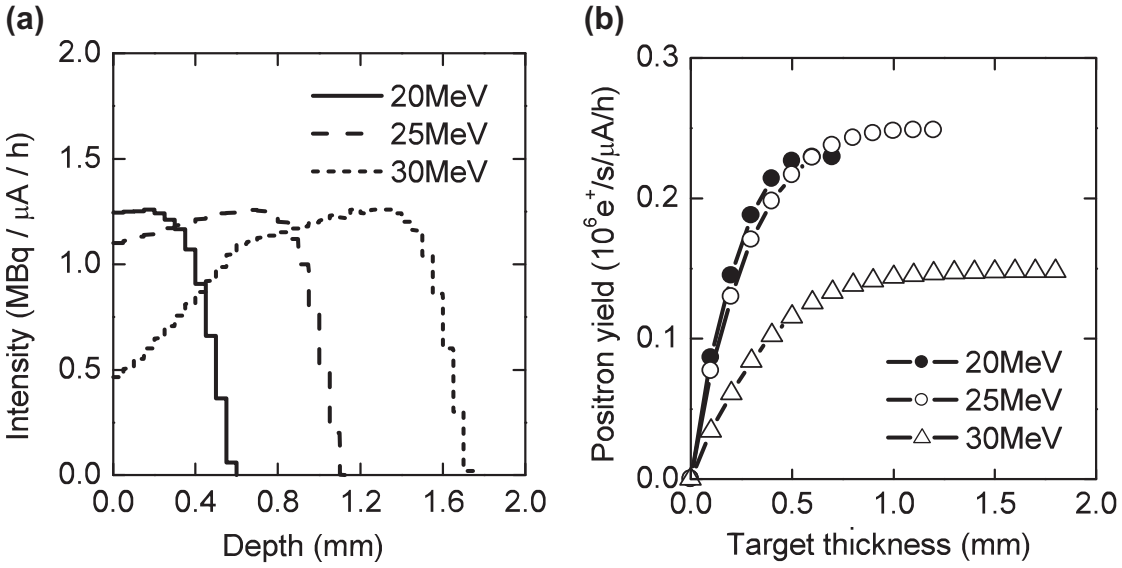

Fig. 2. (a) Simulated depth profiles of ^{68}Ge–^{68}Ga in a GaN target produced by proton bombardment with energies of 20, 25, and 30 MeV. (b) Net positron emission rate from ^{68}Ge–^{68}Ga/GaN as a function of target thickness.

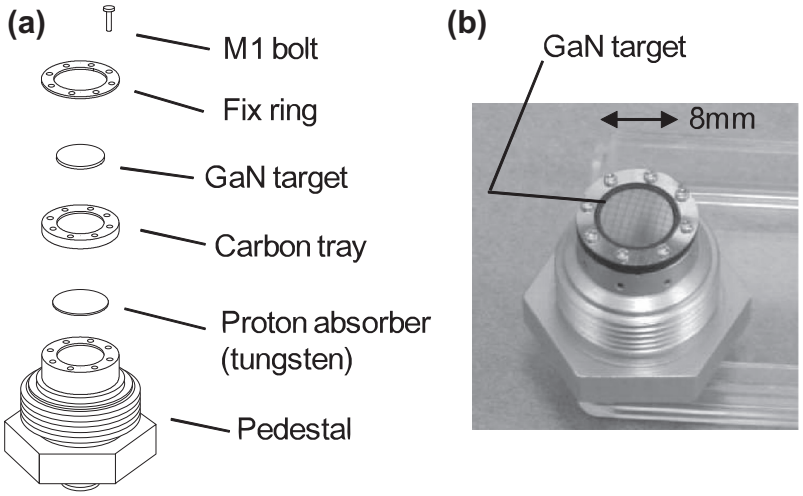

Fig. 3. (a) Schematic and (b) photograph of the source capsule.

energy spectrum. This is in good agreement with the results from our simulation. An additional photopeak was detected at 1.07 MeV with a half-life of 280 days, which was attributed to one of the gamma rays from ^{68}Ga. The irradiation was carried out over 400 h in total in 20 sessions. The irradiation did not cause any significant physical changes, indicating GaN is sufficiently durable as a target material. Fig. 4 shows the net source activity as a function of the elapsed irradiation time.

3.2. Beam generation

To maintain the spin polarization of positrons during the beam transportation, an electrostatic system was used because the positron spin polarization is easily destroyed even by weak magnetic fields. Electrostatic beam transportation can also be used when a controllable magnetic field is applied to a sample. Fig. 5 shows an overview of the positron beam apparatus. The GaN target was moved to the positron gun position after irradiation. The positrons emitted from the GaN target were moderated by a tungsten-mesh moderator composed of 33 tungsten meshes with a wire diameter of 10 μm. [18]. To improve the efficiency, a tungsten ring and tungsten foils (25 μm thick) were added (Fig. 5). The moderator assembly was annealed by an electron beam above 1800 °C for 1 h in a vacuum. The slow positrons were extracted by an extraction grid and focused by a modified SOA gun [19–21] (Fig. 5). The slow positron beam was transported approximately 2 m by nine einzel lenses to a measurement chamber. The longitudinally polarized beam was bent 90° using a magnetic or electrostatic deflector. The magnetic deflector produced a longitudinally polarized beam, whereas the electrostatic deflector produced a transversely polarized beam. The beam was transported with an energy of 5–15 keV. The final beam energy was adjusted using a deceleration/acceleration tube installed in the measurement chamber.

Consequently, a positron beam with a diameter of 5 mm and a flux of 5×10^3 e^+/s was obtained. This flux was consistent with the value derived from the source intensity (200 MBq), the escape efficiency from the GaN target (~0.1) and the remoderation efficiency (2×10^{-4}).

3.3. Spin polarization

The spin polarizations of the ^{68}Ge–^{68}Ga/GaN source and the positron beam were determined from the magnetic quenching of the positronium in fused silica. The para-positronium annihilation probability increases in the magnetic field because of the mixing with the ortho-positronium of the zero magnetic quantum number. The para-positronium annihilation probability is asymmetric upon field reversal; the asymmetry can be used to determine the spin polarization of the positrons. This method was first demonstrated by Nagashima et al. using ACAR [22]. They reported that the precision of this method was 18% compared to 5% for the lifetime method. Nagai et al. showed that positron spin polarization can be determined using DBAR measurements [23]. Furthermore, Hirade developed a similar method based on the ortho-positronium annihilation lifetime observed in polymers [24].

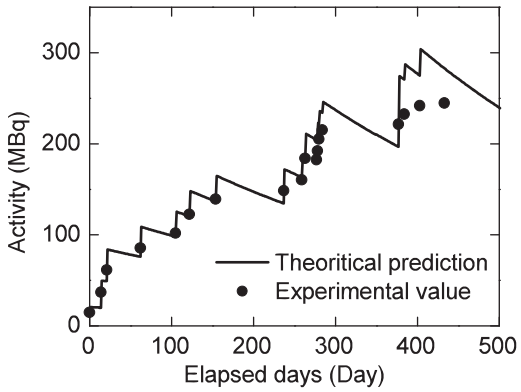

Fig. 4. Net source activity as a function of the elapsed time.

Fig. 7 shows the polarimeter, which consisted of a cylindrical neodymium magnet (diameter: 22.5 mm; magnetic fields: 0.25 or 0.55 T) and a return yoke with a cross section of 10 × 30 mm. The magnetic field could be changed to 0, ±0.25 T and ±0.55 T at the sample position by changing the permanent magnet. Fig. 8 shows the S parameters of fused silica, observed using the ^{68}Ge–^{68}Ga/GaN source and the positron beam with an incident positron energy of 15 keV, as a function of the magnetic field. The distance between the source and the fused silica was 7 mm. These results were fitted with the following equation:

$$I_{Ps} = \frac{\kappa\gamma_p y^2}{\Gamma_{o'}(1+y^2)} F_{o'} + \frac{\kappa\gamma_p}{\Gamma_{p'}(1+y^2)} F_{p'}, \tag{11}$$

$$\Gamma_{o'} = \kappa \frac{\gamma_o + y^2\gamma_p}{1+y^2} + \gamma_{pickoff}, \tag{12}$$

$$\Gamma_{p'} = \kappa \frac{y^2\gamma_o + \gamma_p}{1+y^2} + \gamma_{pickoff}, \tag{13}$$

$$F_{o'} = \frac{(1+y)^2(1-P) + (1-y)^2(1+P)}{8(1+y^2)}, \tag{14}$$

$$F_{p'} = \frac{(1-y)^2(1-P) + (1+y)^2(1+P)}{8(1+y^2)}, \tag{15}$$

$$S = \alpha I_{Ps} + \beta, \tag{16}$$

where I_{Ps} is the para-positronium annihilation intensity, $\Gamma_{o'}$ and $\Gamma_{p'}$ are the total annihilation rates of perturbed para- and ortho-positronium, κ (=0.95) is the contact density, γ_p (=8 ns^{-1}) and γ_o (=0.007 ns^{-1}) are the self-annihilation rates of para- and ortho-positronium in a vacuum, $\gamma_{pickoff}$ (=0.663 ns^{-1}) is the pick-off annihilation rate of ortho-positronium, and α and β are constants. y is given by $y = x/[(1+x^2)^{1/2}+1]$ with $x = 4\mu B/(\kappa E_{hf})$, where μ is the Bohr magneton, B is the magnetic field, E_{hf} is the hyperfine splitting energy of positronium. With P, α, and β as free fitting parameters, the spin polarizations of the source and the beam were determined to be 65 ± 3% and 47 ± 8%, respectively. The spin polarization obtained for the source was in good agreement with that predicted from the maximum spin polarization for the source (92%) and the open angle (55°). The spin polarization of the beam was several percent smaller than that calculated in subsection 2.1. This discrepancy may be caused by depolarization, for example, at the edge of the magnetic deflector and at the entrance of the pole piece. This spin polarization was much higher than for the ^{58}Co (20%) and ^{22}Na (30%) sources without absorbers [5,6,25]. Gidley reported a maximum spin polarization of 66 %, which was obtained by using a ^{22}Na source with a special MgO-smoked tungsten moderator and absorbers, although the beam flux was reduced [4]. Thus, it is important to use positron sources with higher energy end-points to generate highly spin-polarized positron beam.

3.4. DBAR on ferromagnetic Fe

The field-reversal asymmetry of the DBAR spectra for ferromagnetic Fe [26–30] was measured using the ^{68}Ge–^{68}Ga/GaN source and the positron beam. The sample was a polycrystalline Fe ($15 \times 15 \times 2$ mm^3) that was mechanically and electrochemically

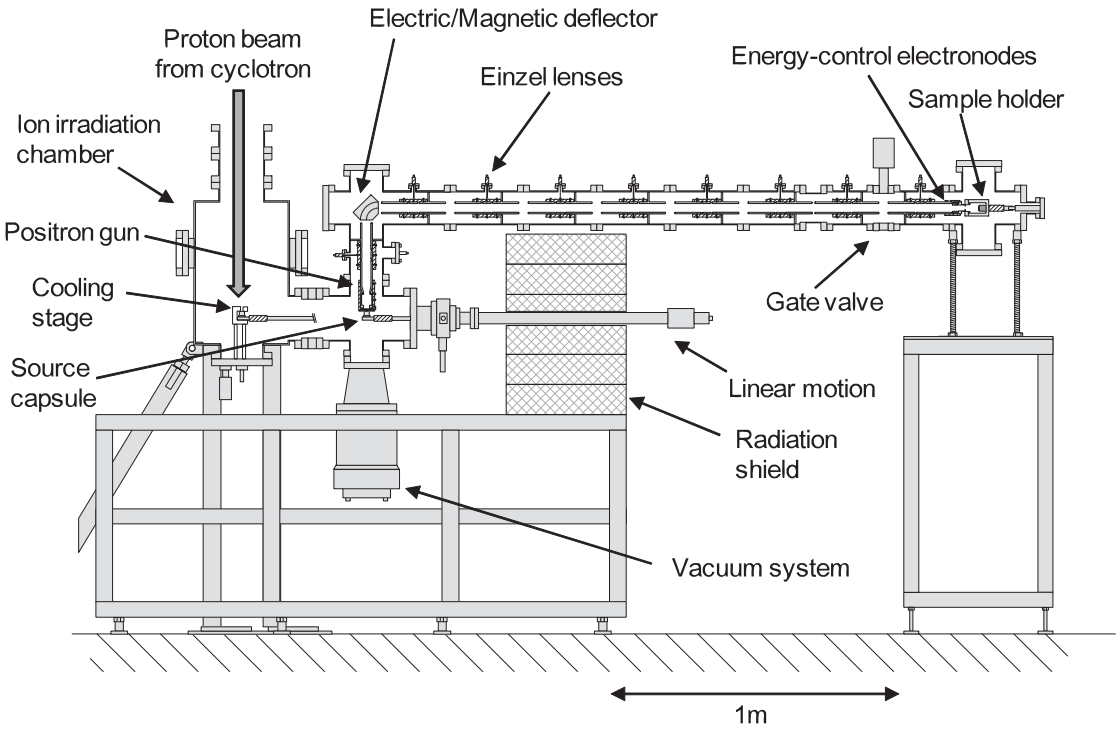

Fig. 5. Schematic of the spin-polarized positron beam line.

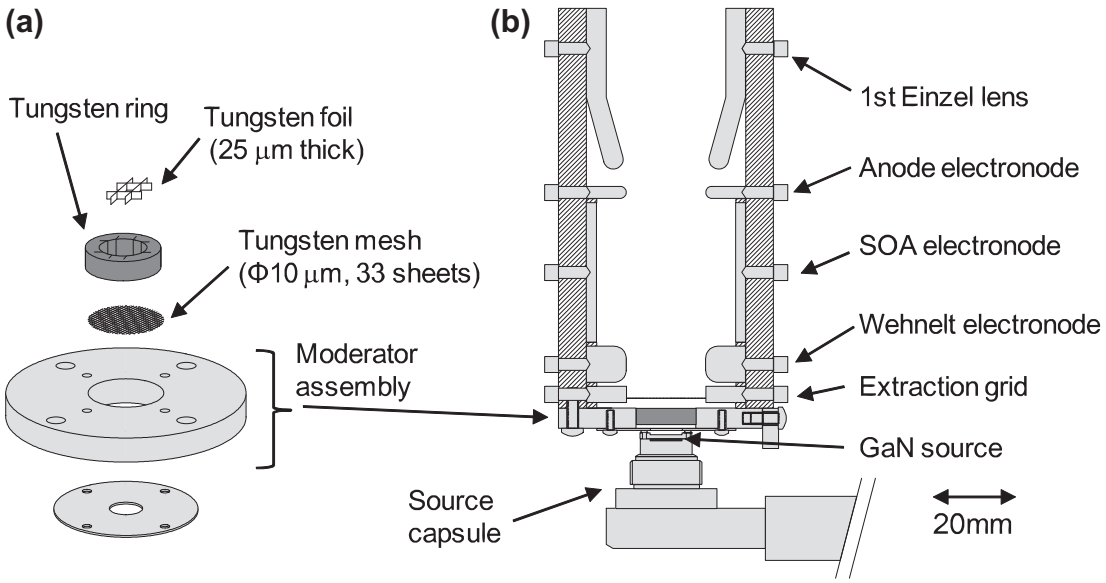

Fig. 6. Schematic of (a) the moderator assembly and (b) the positron gun.

polished and heat-treated at 1150 °C for 2 h in a vacuum. The differential DBAR spectra [$N_{\uparrow}(p)$ and $N_{\downarrow}(p)$] were obtained by altering the field polarity. The subscript ↑ or ↓indicates whether the positron polarization and the magnetic field direction was parallel or antiparallel. The total spectrum area contained more than 1×10^6 events and the intensities were normalized to unity.

Fig. 9 shows the differential DBAR spectra in a magnetic field of 0.55 T. A photon energy of $E_{\gamma} = 1$ keV corresponded to an electron momentum of $p = 3.92 \times 10^3 m_0 c$. The finite differential intensity means that there is a field-reversal asymmetry, which arise from the enhanced annihilation between the spin-up positrons and spin-down 3*d* unpaired electrons [31–33]. The amplitudes of the differential DBAR spectra obtained using the source and the beam were similar. This also shows that our positron beam was sufficiently spin-polarized.

4. Summary

We produced a ^{68}Ge–^{68}Ga source by irradiating a GaN target with high-energy protons. The ^{68}Ge–^{68}Ga activity was increased by repeating the irradiation. A spin-polarized positron beam was then generated using the source. Measurements of the DBAR spectra of fused silica and ferromagnetic Fe in magnetic field demonstrated that the beam was sufficiently spin-polarized.

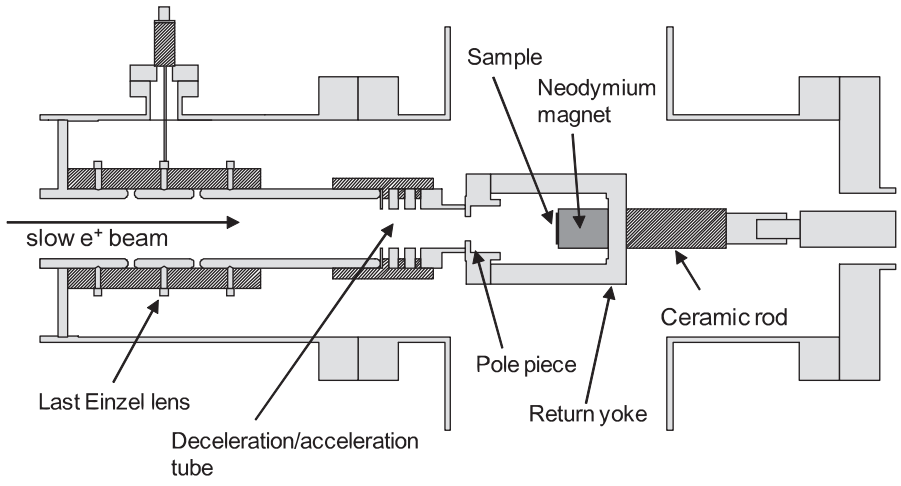

Fig. 7. Schematic of the polarimeter in the chamber.

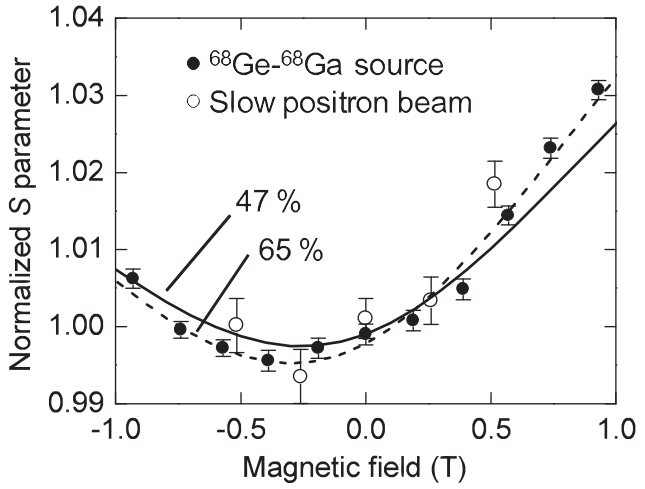

Fig. 8. Magnetic field dependences of S parameters of fused silica obtained using the ^{68}Ge–^{68}Ga source and a slow positron beam (E = 15 keV). Solid and broken lines denote the fitting curves calculated from Eqs. (11)–(16).

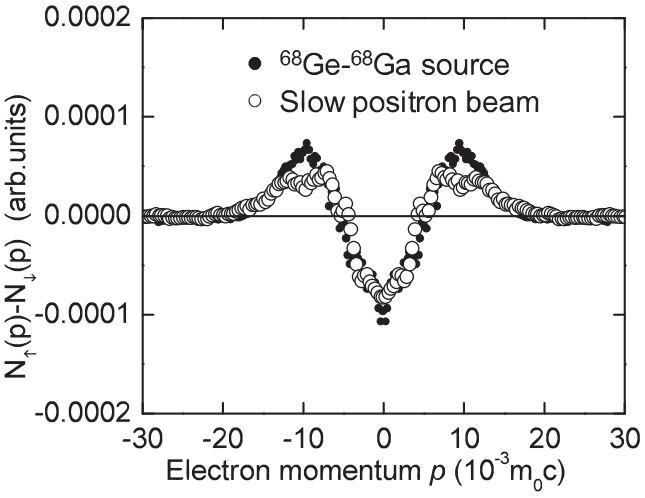

Fig. 9. Differential DBAR spectra of Fe samples obtained in an external magnet field of 0.55 T. This spectrum is folded at p = 0 to enhance the statistics.

Acknowledgment

This work was supported by JSPS KAKENHI Grant No. 24310072.

References

[1] S.S. Hanna, R.S. Preston, Phys. Rev. 106 (1957) 1363–1364.
[2] S. Berko, Positron annihilation in ferromagnetic solids, in: A.T. Stewart, L.O. Roellig (Eds.), Positron Annihilation, Academic Press, 1967, pp. 61–80.
[3] R.S. Preston, S.S. Hanna, Phys. Rev. 110 (1958) 1406–1408.
[4] D.W. Gidley, A.R. Köymen, T.W. Capehart, Phys. Rev. Lett. 49 (1982) 1779–1783.
[5] P.W. Zitzewitz, J.C.V. House, A. Rich, D.W. Gidley, Phys. Rev. Lett. 43 (1979) 1281–1284.
[6] A. Kawasuso, M. Maekawa, Appl. Surf. Sci. 255 (2008) 108–110.
[7] P.G. Coleman, A. Kallis, J. Phys. Conf. Ser. 262 (2011) 012016.
[8] A. Rich, J.V. House, D.W. Gidley, R.S. Conti, Appl. Phys. A 43 (1987) 275–281.
[9] A. Rich, R.S. Conti, D.W. Gidley, M. Skalsey, J.V. House, P. Zitzewitz, Hyperfine Interact. 44 (1988) 125–138.
[10] T. Kumita, M. Chiba, R. Hamatsu, M. Hirose, T. Hirose, H. Iijima, M. Irako, N. Kawasaki, Y. Kurihara, T. Matsumoto, H. Nakabushi, T. Omori, Y. Takeuchi, M. Washio, J. Yang, Appl. Surf. Sci. 116 (1997) 1–6.
[11] T. Nakajyo, M. Tashiro, T. Koizumi, I. Kanazawa, F. Komori, Y. Ito, Appl. Surf. Sci. 116 (1997) 168–176.
[12] J.H. Kim, F. Saito, Y. Nagashima, T. Kurihara, A. Goto, Y. Itoh, T. Hyodo, Radiat. Phys. Chem. 58 (2000) 759–762.
[13] L.A. Page, Rev. Mod. Phys. 31 (1959) 759–781.
[14] A. Vehanen, J. Mäikinen, Appl. Phys. A 36 (1985) 97–101.
[15] E. Beck, Nucl. Instr. Meth. A 76 (1969) 77–84.
[16] Decay Data Evaluation Project Data, DDEP, 2008. Available at: <www.nucleide.org/DDEPWG/DDEPdata.htm>.
[17] S. Tanaka, M. Fukuda, K. Nishimura, JAERI-Data-Code 97-019, 1997, pp. 1–91.
[18] F. Saito, Y. Nagashima, L. Wei, Y. Itoh, A. Goto, T. Hyodo, Appl. Surf. Sci. 194 (2002) 13–15.
[19] F.J. Mulligant, M.S. Lubel, Meas. Sci. Technol. 4 (1993) 197–203.
[20] M. Weber, A. Schwab, D. Becker, K.G. Lynn, Hyperfine Interact. 73 (1992) 147–157.
[21] K.F. Canter, in: A.P. Mills, Jr., W.S. Crane, K.F. Canter (Eds.), Positron Studies of Solids and Surfaces and Atoms, World Scientific, Singapore, 1986, p. 102.
[22] Y. Nagashima, T. Hyodo, Phys. Rev. B 41 (1990) 3937–3941.
[23] Y. Nagai, Y. Nagashima, J. Kim, Y. Itoh, T. Hyodo, Nucl. Instr. Meth. B 171 (2000) 199–203.
[24] T. Hirade, Mater. Sci. Forum 445–446 (2004) 234–238.
[25] D.B. Cassidy, V.E. Meligne, J.A.P. Mills, Phys. Rev. Lett. 104 (2010) 173401.
[26] S.S. Hanna, R.S. Preston, Phys. Rev. 109 (1958) 716–720.
[27] P.E. Mijnarends, Physica 63 (1973) 248–262.
[28] S. Berko, J. Zuckerman, Phys. Rev. Lett. 13 (1964) 339–341.
[29] A. Kawasuso, M. Maekawa, Y. Fukaya, A. Yabuuchi, I. Mochizuki, Phys. Rev. B 83 (2011) 100406(R).
[30] A. Kawasuso, M. Maekawa, Y. Fukaya, A. Yabuuchi, I. Mochizuki, Phys. Rev. B 85 (2011) 024417.
[31] T.W. Mihalisin, R.D. Parks, Phys. Lett. 21 (1966) 610–611.
[32] N. Shiotani, T. Okada, H. Sekizawa, T. Mizoguchi, T. Karasawa, J. Phys. Soc. Jpn. 35 (1973) 456–460.
[33] P. Genoud, A.K. Singh, A.A. Manuel, T. Jarlborg, E. Walker, M. Peter, M. Weller, J. Phys. F 18 (1988) 1933–1947.